Print ISSN : 0022-2755
Journal of Mines, Metals and Fuels
Contents available at: www.informaticsjournals.com/index.php/jmmf

Effects of Uniform and Non-Uniform Temperature Gradients on Marangoni Convection in a Composite layer with Variable Heat Sources

Sumithra. R, Archana. M. A.*, and Deepa. R. Acharya

Department of UG, PG Studies and Research in Mathematics, Government Science College Autonomous, Bengaluru, Karnataka, India. e-mail: sumitra_diya@yahoo.com / archanamurthy78@gmail.com / deeparacharya24@gmail.com

Abstract:

An investigation is carried out to determine the effect of uniform and non-uniform temperature profiles on single component Darcy-Benard Marangoni (DBM) convection in a composite layer system consisting of an incompressible fluid saturated porous layer on top of which is a layer of the same fluid with variable heat sources in both layers. The upper surface of the fluid layer is free with surface tension effects depending on temperature and the lower surface of the porous layer is rigid. The eigen value, thermal Marangoni number (TMN) is solved exactly for linear, parabolic and inverted parabolic temperature profiles for the adiabatic thermal boundary conditions at the horizontal boundaries of the composite layer. The influence of various dimensionless parameters on the eigen value against depth ratio is discussed in detail.

Keywords: *Marangoni convection, Eigen value, Variable heat source, non-uniform temperature profiles.*

1. Introduction

Marangoni convection, the surface tension driven convection has attracted the interest of many researchers. It has applications in the fields of welding, drying silicon wafers, spreading of thin films, nucleation vapor bubbles, material science, aerospace, solid matrix heat exchangers, growth of crystals, manufacturing of semiconductor device, various extractions, and so on. Maragoni convection was first theoretically analyzed by Pearson [5]. Shah and Andras Szeri [8] studied Marangoni instability for non-linear temperature profiles with of non-uniform heat source. Riahi [7] investigated the stability of linear and nonlinear steady convection with a non-uniform internal heat source. Mokthar et al. [2] theoretically analyzed the Marangoni instabilities in case of heat generation in a composite layer. Ramachandramurthy and Aruna [8] studied the Rayleigh-Benard-Taylor instabilities considering variable heat source.

The instabilities of the Marangoni convection have been investigated in many previous works. The Rayleigh-Ritz approach was used by Rudraiah and Siddheshwar [3] to compare the effects of six non-linear temperature gradients with suspended particles on the onset of Marangoni convection. Shivakaumara et al. [9] examined the influence of several fundamental temperature gradients by considering ferrofluids on the onset of Rayleigh-Benard-Marangoni convection. A stability analysis of various basic temperature distributions, with free-slip boundary condition, on the onset of Marangoni convection has been studied by Siti Suzilliana Putri Mohamed Isa et al. [11]. Shivakumara et al. [10] investigated the effects of various non-uniform temperature profiles on

*Corresponding Author

Marangoni convection with the solid plate at the lower surface. Kuznetsov and Nield [1, 4] investigated the onset of natural convection varying the source strength varies by using linear instabilities in a fluid layer and a porous matrix. Recently, Vanishree et al. [16] have studied the effects of linear and non linear temperature gradients on Benard-Marangoni convection with constant heat source in a composite layer. Sumithra et al. [12, 13, 14, 15] have studied the linear stability analysis of Marangoni convection in a composite layer with constant/ temperature dependent heat sink or source for the Darcy and Darcy-Brinkman cases.

The effects of linear, parabolic, and inverted parabolic temperature profiles on the onset of Marangoni convection in a composite system with temperature-dependent heat sources in both the fluid and porous layers are investigated in the current study. The effects of the internal Rayleigh numbers, the ratio of diffusivity, the Darcy number and the horizontal wave number on the onset of DBM convection are illustrated graphically.

2. Mathematical demonstration

Consider an infinite incompressible horizontal fluid layer of depth 'd' overlying a porous layer of depth 'd_m' that contains heat sources Q_{r1} and Q_m respectively. We take a Cartesian coordinate system with the origin at the contact of the fluid and the porous layers, z-axis directed vertically upwards. The fluid layer is bounded by the region $0 \le z \le d$ and the porous layer is bounded by the region $-d_m \le z_m \le 0$. The lower surface of the porous medium is rigid, while the top surface of the fluid layer is free, with surface tension gradients. The heat flux at both boundaries is assumed to be constant.

The basic governing equations are (refer [14]):

$$\nabla \cdot \vec{q}_{r1} = 0 \qquad \text{... (1)}$$

$$\rho_o \left[\frac{\partial \vec{q}_{r1}}{\partial t} + \left(\vec{q}_{r1} \cdot \nabla \right) \vec{q}_{r1} \right] = -\nabla P_{r1} + \mu \nabla^2 \vec{q}_{r1} \qquad \text{... (2)}$$

$$\frac{\partial T}{\partial t} + \left(\vec{q}_{r1} \cdot \nabla \right) T = \kappa \nabla^2 T + Q_{r1} \left(T - T_o \right) \qquad \text{... (3)}$$

$$\nabla_m \cdot \vec{q}_m = 0 \qquad \text{... (4)}$$

$$\frac{\rho_0}{\phi} \frac{\partial \vec{q}_m}{\partial t_m} = -\nabla_m P_m - \frac{\mu}{K} \vec{q}_m \qquad \text{... (5)}$$

$$A \frac{\partial T_m}{\partial t} + \left(\vec{q}_m \cdot \nabla_m \right) T_m = \kappa_m \nabla^2 T_m + Q_m \left(T_m - T_o \right) \qquad \text{... (6)}$$

where $\vec{q}_{r1} = (u_{r1}, v_{r1}, w_{r1})$ represents velocity vector for the fluid layer and $\vec{q}_m = (u_m, v_m, w_m)$ represents velocity vector for the porous medium, ϕ is the porosity, ρ_o represents fluid density, μ represents fluid viscosity, P_{r1} is the pressure, K - the permeability of the porous medium, κ - the thermal diffusivity of the fluid, $A = \frac{\left(\rho c_p\right)_m}{\left(\rho c_p\right)_{r1}}$ represents ratio of heat capacities, c_p - the specific heat, t - the time, T denotes temperature in the fluid layer, T_m denotes temperature porous layer. Here the suffix 'm' denotes the quantities in the porous layer, '$r1$' denotes the quantities in the fluid layer. The fundamental steady state is assumed to be quiescent, and the solution is as follows:

$$\left[\vec{q}_{r1}, P_{r1}, T \right] = \left[0, P_{r1_b}\left(z\right), T_b\left(z\right) \right] \qquad \text{... (7)}$$

$$\left[\vec{q}_m, P_m, T_m \right] = \left[0, P_{mb}\left(z_m\right), T_{mb}\left(z_m\right) \right] \qquad \text{... (8)}$$

The subscript 'b' refers to the basic state.

The basic state temperatures $Tb(z)$ and $T_{mb}(z_m)$ are (refer [14]):

$$T_b\left(z\right) = T_o + \frac{(T_u - T_o)}{\sin\left(\sqrt{\frac{Q_{r1}}{\kappa}} d\right)} \sin\left(\sqrt{\frac{Q_{r1}}{\kappa}} z\right) f(z), \;\; 0 \le z \le d \qquad \text{... (9)}$$

$$T_{mb}\left(z_m\right)=T_o+\frac{(T_o-T_L)}{\sin\left(\sqrt{\frac{Q_m}{\kappa_m}}d_m\right)}\sin\left(\sqrt{\frac{Q_m}{\kappa_m}}z_m\right)f_m\left(z_m\right),\ -d_m\le z_m\le 0 \quad \text{... (10)}$$

$$\text{where, } T_o=\frac{T_u\sqrt{Q_{r1}\kappa}\sin\left(\sqrt{\frac{Q_m}{\kappa_m}}d_m\right)+T_L\sqrt{Q_m\kappa_m}\sin\left(\sqrt{\frac{Q_{r1}}{\kappa}}d\right)}{\sqrt{Q_m\kappa_m}\sin\left(\sqrt{\frac{Q_{r1}}{\kappa}}d\right)+\sqrt{Q_{r1}\kappa}\sin\left(\sqrt{\frac{Q_m}{\kappa_m}}d_m\right)}$$

is the interface temperature, $f(z)$ and $f_m(z_m)$ are the dimensionless temperature profiles in the fluid and the porous medium respectively.

Following Sumithra *et al*.[14], the basic solution is perturbed, linearized, non-dimensionalized by taking suitable scale lengths in both the layers. After subject to normal mode analysis, differential equations so obtained are (refer [14]):

$$\left(D^2-a^2\right)\left(D^2-a^2-\frac{n}{\Pr}\right)W\left(z\right)=0 \quad \text{... (11)}$$

$$\left(\frac{n_m\beta^2}{\Pr_m}-1\right)\left(D_m{}^2-a_m{}^2\right)W_m\left(z_m\right)=0 \quad \text{... (12)}$$

$$\left(D^2-a^2+R_I+n\right)\Theta\left(z\right)+\frac{\sqrt{R_I}\cos\left(\sqrt{R_I}z\right)}{\sin\sqrt{R_I}}W\left(z\right)f\left(z\right)=0 \quad \text{... (13)}$$

$$\left(D_m{}^2-a_m{}^2+R_{I_m}+n_mA\right)\Theta_m(z_m)+W_m\left(z_m\right)\sqrt{R_{I_m}}\frac{\cos\left(\sqrt{R_{I_m}}z_m\right)}{\sin\sqrt{R_{I_m}}}f_m\left(z_m\right)=0 \quad \text{... (14)}$$

where $Da=\frac{K}{d_m{}^2}=\beta^2$ represents the Darcy number, $R_I=\frac{Q_{r1}}{\kappa}d^2$ and $R_{I_m}=\frac{Q_m}{\kappa_m}d_m{}^2$ respectively are the fluid and porous internal Rayleigh numbers, $\Pr=\frac{\mu}{\rho_o\kappa}$ and $\Pr_m=\frac{\phi\mu}{\rho_o\kappa_m}$ are the Prandtl numbers in the fluid and the porous layers respectively, a and a_m are the wave numbers in the fluid and porous layers, W_m and W are the vertical components of the velocity vectors in the porous and fluid layers. Considering the steady state convection, i.e., $n = n_m = 0$, the equations (11) to (14) reduces to

$$\left(D^2-a^2\right)^2W\left(z\right)=0 \quad \text{... (15)}$$

$$\left(D_m{}^2-a_m{}^2\right)W_m\left(z_m\right)=0 \quad \text{... (16)}$$

$$\left(D^2-a^2+R_I\right)\Theta\left(z\right)=-\frac{\sqrt{R_I}\cos\left(\sqrt{R_I}z\right)}{\sin\sqrt{R_I}}W\left(z\right)f\left(z\right) \quad \text{... (17)}$$

$$\left(D_m{}^2-a_m{}^2+R_{I_m}\right)\Theta_m(z_m)=-W_m\left(z_m\right)\sqrt{R_{I_m}}\frac{\cos\left(\sqrt{R_{I_m}}z_m\right)}{\sin\sqrt{R_{I_m}}}f_m\left(z_m\right) \quad \text{... (18)}$$

3. Boundary conditions

The associated boundary conditions are non-dimensionalized and subjected to normal mode analysis. (Refer Sumithra et al. [14]):

$$W(1)=0 \quad \text{... (19)}$$

$$D^2W(1)+M\Theta(1)a^2=0 \quad \text{... (20)}$$

$$D\Theta(1)=0 \quad \text{... (21)}$$

$$W_m(0)=\frac{\varepsilon_T}{\zeta}W(0) \quad \text{... (22)}$$

$$\left(D^2+a^2\right)W(0)=\frac{\zeta^3}{\varepsilon_T}\left(D_m{}^2+a_m{}^2\right)W_m(0) \quad \text{... (23)}$$

$$\Theta(0)=\frac{\varepsilon_T}{\zeta}\Theta_m(0) \quad \text{... (24)}$$

$$D\Theta(0)=D_m\Theta_m(0) \quad \text{... (25)}$$

$$\left(D^3-3a^2D\right)W(0)=-\frac{\zeta^4}{Da\,\varepsilon_T}D_mW_m(0) \quad \text{... (26)}$$

$$W_m(-1)=0 \quad \text{... (27)}$$

$$D_m\Theta_m(-1)=0 \quad \text{... (28)}$$

Here $M=-\frac{\partial\sigma}{\partial T}\frac{(T_o-T_u)d}{\mu\kappa}$ represents the thermal Marangoni number, σ represents surface tension and T_u is the temperature at the upper layer of the fluid, $\zeta=\frac{d}{d_m}$ is the depth ratio and $\varepsilon_T=\frac{\kappa}{\kappa_m}$ represents the ratio of thermal diffusivities.

4. Method of solution

The equations (15) and (16) are independent of temperatures $\Theta(z)$ and $\Theta_m(z_m)$. We use boundary conditions (19), (22), (23), (26), (27) to obtain $W(z)$ and $W_m(z_m)$.

$$W(z)=A_1\left[A_2\sinh(az)+A_3z\cosh(az)+A_4z\sinh(az)+\cosh(az)\right] \quad \text{... (29)}$$

$$W_m(z_m)=\frac{\varepsilon_T}{\zeta}A_1\left[\cosh(a_mz_m)+\sinh(a_mz_m)\coth(a_m)\right] \quad \text{... (30)}$$

$$A_2=\frac{\zeta a_m\cosh(a_m)}{2a^3Da\sinh(a_m)},\quad A_3=-\left[1+(A_2+A_4)\tan ha\right],\quad A_4=\frac{\zeta^2a_m{}^2}{a}-a$$

Equations (17) and (18), along with the boundary conditions (19–28), form an eigen value problem with the Marangoni number as an eigen value. The current study aims to comprehend the stability of the composite system using various basic temperature profiles, such as $f(z)=f_m(z_m)=1$ for the linear, $f(z)=2z$, $f_m(z_m)=2z_m$ for the parabolic, and $f(z)=(2-2z)$, $f_m(zm)=(2-2z_m)$ for the inverted parabolic profile.

4.1. Linear temperature profile

Considering the linear case [refer 14], i.e.,

$$f(z)=f_m(z_m)=1 \quad \text{... (31)}$$

By substituting (31) in equations (17) and (18), and solving for $\Theta(z)$ and $\Theta_m(z_m)$ temperature boundary conditions (21), (24), (25) and (28), we get,

$$\Theta(z)=A_1\left[c_{f2}\sinh(bz)+c_{f1}\cosh(bz)-h(z)\right] \quad \text{... (32)}$$

$$\Theta_m(z_m)=A_1\left[c_{3p}\cosh(b_m z_m)+c_{4p}\sinh(b_m z_m)-h_m z_m\right] \quad \text{... (33)}$$

where $b=\sqrt{a^2-R_I}$, $b_m=\sqrt{a_m^{\ 2}-R_{I_m}}$, $h(z)=\dfrac{A_5}{2}\left(I_{f1}+I_{f2}+I_{f3}\right)$

$$h_m(z_m)=\frac{\varepsilon_T A_6}{2\zeta}\left(\sinh(a_m z_m)\sin\left(\sqrt{R_{I_m}}z_m\right)+\coth(a_m)\cosh(a_m z_m)\sin\left(\sqrt{R_{I_m}}z_m\right)\right).$$

$$c_{f1}=\delta_1+\frac{\varepsilon_T}{\zeta}c_{3p},\quad c_{f2}=\frac{\delta_3-c_{f1}b\sinh b}{b\cosh b},\quad c_{4p}=\frac{c_{3p}b_m\sinh b_m}{b_m\cosh b_m}$$

$$c_{3p}=\frac{\delta_4\cosh b+\delta_3\cosh b_m-b\delta_1\cosh b_m\sinh b-\delta_2\cosh b_m\cosh b}{b_m\sinh b_m\cosh b+\dfrac{\varepsilon_T}{\zeta}b\sinh b\cosh b_m}$$

$$I_{f1}=\sin\left(\sqrt{R_I}z\right)\left[\sinh(az)+A_2\cosh(az)\right],$$

$$I_{f2}=A_3\left[\left(z\sinh(az)-\frac{1}{a}\cosh(az)\right)\sin\left(\sqrt{R_I}z\right)+\frac{1}{\sqrt{R_I}}\cos\left(\sqrt{R_I}z\right)\sinh(az)\right],$$

$$I_{f3}=A_4\left[\left(z\cosh(az)-\frac{1}{a}\sinh(az)\right)\sin\left(\sqrt{R_I}z\right)+\frac{1}{\sqrt{R_I}}\cos\left(\sqrt{R_I}z\right)\cosh(az)\right]$$

$$\delta_1=\frac{A_5A_4}{2\sqrt{R_I}},\quad \delta_2=\left(\frac{A_5\sqrt{R_I}}{2}\right)\left(A_2-\frac{A_3}{a}+\frac{aA_3}{R_I}\right)-\left(\frac{A_6\varepsilon_T\sqrt{R_{I_m}}\coth a_m}{2\zeta}\right)$$

$$\delta_3=\frac{A_5}{2}\left(\Lambda_1+A_2\Lambda_2+A_3\Lambda_3+A_4\Lambda_4\right),\quad \delta_4=\frac{A_6\varepsilon_T}{2\zeta}\left(\lambda_1-\lambda_2\coth a_m\right)$$

$$\Lambda_1=a\cosh a\sin\sqrt{R_I}+\sqrt{R_I}\sinh a\cos\sqrt{R_I},\quad \Lambda_2=a\sinh a\sin\sqrt{R_I}+\sqrt{R_I}\cosh a\cos\sqrt{R_I}$$

$$\Lambda_3=\Lambda_{13}-\Lambda_{23},\ \Lambda_{13}=a\sin\sqrt{R_I}\cosh a+\sqrt{R_I}\cosh a\cos\sqrt{R_I}-\frac{1}{a}\sqrt{R_I}\cos\sqrt{R_I}\cosh a$$

$$\Lambda_4=\Lambda_{41}+\Lambda_{42},\quad \Lambda_{41}=a\sin\sqrt{R_I}\sinh a+\cosh a\left(\sqrt{R_I}\cos\sqrt{R_I}-\sin\sqrt{R_I}\right)$$

$$\Lambda_{42}=-A_7\cos\sqrt{R_I}\sinh a,\quad \lambda_2=a_m\sinh a_m\sin\sqrt{R_{I_m}}+\sqrt{R_{I_m}}\cosh a_m\cos\sqrt{R_{I_m}}$$

$$\lambda_1=a_m\cosh a_m\sin\sqrt{R_{I_m}}+\sqrt{R_{I_m}}\sinh a_m\cos\sqrt{R_{I_m}},\ \Lambda_{23}=\sin\sqrt{R_I}\sinh a-\frac{a}{\sqrt{R_I}}\cos\sqrt{R_I}\cosh a$$

For the linear profile, the TMN, M_L is,

$$M_L=-\frac{D^2W(1)}{a^2\Theta(1)}=-\frac{m_{11}\cosh a+m_{12}\sinh a}{a^2\left(m_{21}+A_3m_{22}+A_4m_{23}\right)} \quad \text{... (34)}$$

$$m_{11}=a^2\left(1+A_3\right)+2aA_4,\quad m_{12}=a^2\left(A_2+A_4\right)+2aA_3$$

$$m_{21}=c_1\cosh b+c_2\sinh b-\frac{A_5}{2}\left(\sinh a\sin\sqrt{R_I}+A_2\cosh a\sin\sqrt{R_I}\right)$$

$$m_{22}=-\frac{A_5}{2}\left(\sinh a\sin\sqrt{R_I}+\frac{1}{\sqrt{R_I}}\cos\sqrt{R_I}\sinh a-\frac{1}{a}\sin\sqrt{R_I}\cosh a\right)$$

$$m_{23} = -\frac{A_5}{2}\left(\sin\sqrt{R_I}\cosh a - \frac{1}{a}\sin\sqrt{R_I}\sinh a + \frac{1}{\sqrt{R_I}}\cos\sqrt{R_I}\cosh a\right)$$

4.2 Parabolic temperature profile

The equations for this case is,

$$f(z) = 2z, \quad f_m(z_m) = 2z_m \qquad \text{... (35)}$$

By substituting (35) in equations (17) and (18), and solving for $\Theta(z)$ and $\Theta_m(z_m)$ using the temperature boundary conditions (21), (24), (25) and (28), we get,

$$\Theta(z) = A_1\left[c_{p1}\cosh(bz) + c_{p2}\sinh(bz) - h(z)\right] \qquad \text{... (36)}$$

$$\Theta_m(z_m) = A_1\left[c_{p3}\cosh(b_m z_m) + c_{p4}\sinh(b_m z_m) - h_m z_m\right] \qquad \text{... (37)}$$

where $h(z) = A_5\left[I_1 + I_2 + I_3 + I_4\right], \quad h_m(z_m) = \frac{\varepsilon_T A_6}{\zeta}\left[I_{m1} + (\coth a_m)I_{m2}\right]$

$$b = \sqrt{a^2 - R_I}, \; b_m = \sqrt{a_m{}^2 - R_{I_m}}, \; I_1 = [z\sinh(az) - \frac{1}{a}\cosh(az)]\sin(\sqrt{R_I}z) + \frac{1}{\sqrt{R_I}}\sinh(az)\cos(\sqrt{R_I}z)$$

$$I_2 = A_2\left[\left(z\cosh(az) - \frac{1}{a}\sinh(az)\right)\sin\left(\sqrt{R_I}z\right) + \frac{1}{\sqrt{R_I}}\cosh(az)\cos(\sqrt{R_I}z)\right]$$

$$I_3 = A_3\left(I_{31} + I_{32}\right), \; I_{31} = \left(\frac{2z}{\sqrt{R_I}}\sinh(az) - \frac{3}{a\sqrt{R_I}}\cosh(az)\right)\cos\left(\sqrt{R_I}z\right)$$

$$I_{32} = \left(z^2 - \frac{2}{R_I} + \frac{2}{a^2}\right)\sinh(az)\sin\left(\sqrt{R_I}z\right) - \frac{2z}{a}\cosh(az)\sin\left(\sqrt{R_I}z\right)$$

$$I_4 = A_4\left(I_{41} + I_{42}\right), \; I_{41} = \left(\frac{2z}{\sqrt{R_I}}\cosh(az) - \frac{3}{a\sqrt{R_I}}\cosh(az)\right)\cos\left(\sqrt{R_I}z\right)$$

$$I_{42} = \left(z^2 - \frac{2}{R_I} + \frac{2}{a^2}\right)\cosh(az)\sin\left(\sqrt{R_I}z\right) - \frac{2z}{a}\sinh(az)\sin\left(\sqrt{R_I}z\right)$$

$$I_{m1} = \left(z_m\sinh(a_m z_m) - \frac{1}{a_m}\cosh(a_m z_m)\right)\sin\left(\sqrt{R_{I_m}}z_m\right) + \frac{1}{\sqrt{R_{I_m}}}\sinh(a_m z_m)\cos\left(\sqrt{R_{I_m}}z_m\right)$$

$$I_{m2} = \left(z_m\cosh(a_m z_m) - \frac{1}{a_m}\sinh(a_m z_m)\right)\sin\left(\sqrt{R_{I_m}}z_m\right) + \frac{1}{\sqrt{R_{I_m}}}\cosh(a_m z_m)\cos\left(\sqrt{R_{I_m}}z_m\right)$$

$$c_{p1} = \eta 2 + \frac{\varepsilon_T}{\zeta}c_{p3}, \quad c_{p2} = \frac{\eta_1 - c_{p1}b\sinh b}{b\cosh b}, \; c_{p4} = \frac{\eta_3 + bc_{p2}}{b_m}$$

$$c_{p3} = \frac{\eta_1 - (b\eta_2)\cosh b_m \sinh b + (\cosh b)(\eta_3\cosh b_m - \eta_4)}{(\cosh b)(b_m)\sinh b_m + \left(\frac{\varepsilon_T}{\zeta}\right)b\cosh b_m\sinh b}, \; A_7 = \left(\frac{\sqrt{R_I}}{a} - \frac{a}{\sqrt{R_I}}\right)$$

$$\eta_1 = A_5\left(\eta_{11} + A_2\eta_{12} + A_3\left(\eta_{13} + \eta_{23}\right) + A_4\left(\eta_{14} + \eta_{24}\right)\right), \; A_5 = \frac{1}{a\sin\sqrt{R_I}}$$

$$\eta_{11} = \sqrt{R_I}\sinh a\cos\sqrt{R_I} + a\cosh a\sin\sqrt{R_I} - A_7\cosh a\cos\sqrt{R_I} - \sinh a\sin\sqrt{R_I}$$

$$\eta_{12} = \sqrt{R_I}\cosh a\ \cos\sqrt{R_I} + a\sinh a\ \sin\sqrt{R_I} - A_7\sinh a\ \cos\sqrt{R_I} - \cosh a\ \sin\sqrt{R_I}$$

$$\eta_3 = A_5\left[A_4\left(\frac{2\sqrt{R_I}}{a^2} - \frac{3}{\sqrt{R_I}}\right) - A_7\right] - \frac{\varepsilon_T A_6}{\zeta}A_8,\ A_8 = \left(\frac{a_m}{\sqrt{R_{I_m}}} - \frac{\sqrt{R_{I_m}}}{a_m}\right)$$

$$\eta_{13} = \left(\sqrt{R_I} - \frac{3}{\sqrt{R_I}} + \frac{2\sqrt{R_I}}{a^2}\right)\sinh a\ \cos\sqrt{R_I} - 2A_7\cos\sqrt{R_I}\ \cosh a$$

$$\eta_{23} = \left[\cosh a\left(a + \frac{3}{a} - \frac{2a}{R_I}\right) - 2(\sinh a)\right]\sin\sqrt{R_I}$$

$$\eta_{14} = \left(\sqrt{R_I} - \frac{3}{\sqrt{R_I}} + \frac{2\sqrt{R_I}}{a^2}\right)\cosh a\ \cos\sqrt{R_I} - 2A_7\sinh a\ \cos\sqrt{R_I}$$

$$\eta_{24} = \left(a + \frac{3}{a} - \frac{2a}{R_I}\right)\sinh a\ \sin\sqrt{R_I} - 2\cosh a\ \sin\sqrt{R_I},\ A_6 = \frac{1}{a_m\sin\sqrt{R_{I_m}}}$$

$$\eta_2 = A_5\left(\frac{A_2}{\sqrt{R_I}} - \frac{3A_3}{a\sqrt{R_I}}\right) - \frac{\varepsilon_T{}^2 A_6\coth a_m}{\zeta^2\sqrt{R_{I_m}}},\ \eta_4 = \frac{\varepsilon_T A_6}{\zeta}\left(\eta_{41} - \eta_{42}\coth a_m\right)$$

The corresponding TMN, M_{PB} is as follows:

$$M_{PB} = -\frac{D^2W(1)}{a^2\Theta(1)} = -\frac{m_{P1}\cosh a + m_{P2}\sinh a}{a^2\left(m_{P3} - A_5\left[A_2m_{p4} + A_3m_{P5} + A_4m_{P6} + m_{P7}\right]\right)} \quad \text{... (38)}$$

$$m_{P1} = a^2\left(1 + A_3\right) + 2aA_4,\quad m_{P2} = a^2\left(A_2 + A_4\right) + 2aA_3,$$

$$m_{P3} = c_{P1}\cosh b + c_{P2}\sinh b,\ \ m_{P7} = \left[\sinh a - \frac{\cosh a}{a} + \frac{\cosh a}{\sqrt{R_I}}\right]\sin\sqrt{R_I}$$

$$m_{P4} = \left[\cosh a - \frac{\sinh a}{a}\right]\sin\sqrt{R_I} + \frac{\cosh a\ \cos\sqrt{R_I}}{\sqrt{R_I}},\ A_9 = \left(1 - \frac{2}{R_I} + \frac{2}{a^2}\right),$$

$$m_{P5} = \left(\frac{2\sinh a}{\sqrt{R_I}} - \frac{3\cosh a}{a\sqrt{R_I}}\right)\cos\sqrt{R_I} + \left[A_9\sinh a - \frac{2\cosh a}{a}\right]\sin\sqrt{R_I}\ ,$$

$$m_{P6} = \cos\sqrt{R_I}\left(\frac{2\cosh a}{\sqrt{R_I}} - \frac{3\sinh a}{a\sqrt{R_I}}\right) + \left[A_9\cosh a - \frac{2\sinh a}{a}\right]\sin\sqrt{R_I}$$

4.3 Inverted parabolic temperature profile

The functions for this case are as follows:

$$f(z) = (2 - 2z),\ f_m(z_m) = (2 - 2z_m) \quad \text{... (39)}$$

By substituting (39) in equations (17) and (18), and solving for $\Theta(z)$ and $\Theta_m(z_m)$ using the thermal boundary conditions (21), (24), (25) and (28), we get,

$$\Theta(z) = A_1\left[c_1\cosh(bz) + c_2\sinh(bz) - h(z)\right] \quad \text{... (40)}$$

$$\Theta_m(z_m) = A_1\left[c_{mp1}\cosh(b_mz_m) + c_{mp2}\sinh(b_mz_m) - h_mz_m\right] \quad \text{... (41)}$$

where $h(z) = A_5\left[i_1 + i_2 + i_3 + i_4\right]$, $h_m\left(z_m\right) = \frac{\varepsilon_T A_6}{\zeta}\left[i_{m1} + (\coth a_m) i_{m2}\right]$

$$b = \sqrt{a^2 - R_I},\ b_m = \sqrt{a_m{}^2 - R_{I_m}},\ i_1 = \left[\left(1 - z + \frac{1}{a}\right)\sinh(az)\sin\left(\sqrt{R_I}\,z\right) - \frac{\cosh(az)\cos\left(\sqrt{R_I}\,z\right)}{\sqrt{R_I}}\right]$$

$$i_2 = A_2\left[\left(1 - z + \frac{1}{a}\right)\cosh(az)\sin\left(\sqrt{R_I}\,z\right) - \frac{\sinh(az)\cos\left(\sqrt{R_I}\,z\right)}{\sqrt{R_I}}\right],\ i_3 = A_3\left(i_{31} + i_{32}\right)$$

$$i_{31} = \frac{\cos\left(\sqrt{R_I}\,z\right)}{a\sqrt{R_I}}\left[a\left(1 - 2z\right)\sinh(az) + 3\cosh(az)\right],\quad i_4 = A_4\left(i_{41} + i_{42}\right)$$

$$i_{32} = \left[\left(\frac{2}{R_I} - \frac{2}{a^2} + z - z^2\right)\sinh(az) - \frac{\left(1 - 2z\right)\cosh(az)}{a}\right]\sin\left(\sqrt{R_I}\,z\right),\ c_{mp1} = \frac{\zeta}{\varepsilon_T}\left(c_1 - \xi_2\right)$$

$$i_{41} = \frac{\cos\left(\sqrt{R_I}\,z\right)}{a\sqrt{R_I}}\left[a\left(1 - 2z\right)\cosh(az) + 3\sinh(az)\right],\ c_2 = \frac{\xi_1 - c_1\sinh b}{b\cosh b}$$

$$i_{42} = \left[\left(\frac{2}{R_I} - \frac{2}{a^2} + z - z^2\right)\cosh(az) - \frac{\left(1 - 2z\right)\sinh(az)}{a}\right]\sin\left(\sqrt{R_I}\,z\right)$$

$$i_{m1} = \left[\left(1 - z_m + \frac{1}{a_m}\right)\sinh\left(a_m z_m\right)\sin\left(\sqrt{R_{I_m}}\,z_m\right) - \frac{\cosh\left(a_m z_m\right)\cos\left(\sqrt{R_{I_m}}\,z_m\right)}{\sqrt{R_{I_m}}}\right]$$

$$c_{mp2} = \frac{c_2 b - \xi_3}{b_m},\ c_1 = \frac{c_{11}\cosh b_m + c_{12}\cosh b}{b_m(\cosh b)\ \sinh b_m + \frac{\varepsilon_T}{\zeta} b(\sinh b)\ \cosh b_m},\ c_{11} = \frac{\varepsilon_T}{\zeta}\left(\xi_1 - \xi_3\cosh b\right)$$

$$i_{m2} = \left[\left(1 - z_m + \frac{1}{a_m}\right)\cosh\left(a_m z_m\right)\sin\left(\sqrt{R_{I_m}}\,z_m\right) - \frac{\sinh\left(a_m z_m\right)\cos\left(\sqrt{R_{I_m}}\,z_m\right)}{\sqrt{R_{I_m}}}\right]$$

$$c_{12} = \xi_2 b_m \sinh b_m - \frac{\varepsilon_T}{\zeta}\xi_4,\ \xi_2 = A_5\left(\frac{3A_3}{a\sqrt{R_I}} + \frac{A_4}{\sqrt{R_I}} - \frac{1}{\sqrt{R_I}}\right) + \frac{\varepsilon_T{}^2 A_6}{\zeta^2\sqrt{R_{I_m}}}$$

$$\xi_3 = A_5\left[A_2\xi_{31} - A_3 A_7 + A_4\xi_{32}\right] - \frac{\varepsilon_T A_6\coth a_m}{\zeta}\xi_{33},\ \xi_{31} = \sqrt{R_I} + A_7$$

$$\xi_{41} = 2\left(a_m + 1\right)\sinh a_m + \cosh a_m,\ \xi_{42} = 2\sqrt{R_{I_m}} - A_8,\ \xi_{43} = 2\left(a_m + 1\right)\cosh a_m + \sinh a_m$$

$$\xi_{32} = \frac{3}{\sqrt{R_I}} - \frac{2\sqrt{R_I}}{a^2},\ \xi_{33} = \sqrt{R_{I_m}} - A_8,\ \xi_{15} = \left[\left(A_7\sinh a + \frac{3\cosh a}{\sqrt{R_I}} - \frac{2\sqrt{R_I}\cosh a}{a^2}\right)\right]\cos\sqrt{R_I}$$

$$\xi_1 = A_5\left[\xi_{11} + A_2\xi_{12} + A_3\left(\xi_{13} + \xi_{14}\right) + A_4\left(\xi_{15} + \xi_{16}\right)\right],\ \xi_{13} = \left[A_7\cosh a + \frac{3}{\sqrt{R_I}}\sinh a\right]\cos\sqrt{R_I}$$

$$\xi_{11} = A_7 \sinh a \cos\sqrt{R_I} + (2\cosh a - \sinh a)\sin\sqrt{R_I},\ \xi_{14} = \left[\sinh a + \left(\frac{2a}{R_I} - \frac{3}{a}\right)\cosh a\right]\sin\sqrt{R_I}$$

$$\xi_{12} = A_7 \cosh a \cos\sqrt{R_I} + (2\sinh a - \cosh a)\sin\sqrt{R_I},\ \xi_{16} = \left[\cosh a + \left(\frac{2a}{R_I} - \frac{3}{a}\right)\sinh a\right]\sin\sqrt{R_I}$$

$$\xi_4 = \frac{A_6 \varepsilon_T}{\zeta}\left[\coth a_m \left(\xi_{41} \sin\sqrt{R_{I_m}} + \xi_{42} \cosh a_m \cos\sqrt{R_{I_m}}\right) - \left(\xi_{43} \sin\sqrt{R_{I_m}} + \xi_{42} \sinh a_m \cos\sqrt{R_{I_m}}\right)\right]$$

The corresponding TMN, M_{IP} is

$$M_{IP} = -\frac{D^2 W(1)}{a^2 \Theta(1)} = -\frac{m_{I1} \cosh a + m_{I2} \sinh a}{a^2\left(m_{I3} - A_5\left[A_2 m_{I4} + A_3 m_{I5} + A_4 m_{I6} + m_{I7}\right]\right)} \quad \text{... (42)}$$

$$m_{I1} = a^2(1 + A_3) + 2aA_4,\quad m_{I2} = a^2(A_2 + A_4) + 2aA_3,\quad m_{I3} = c_1 \cosh b + c_2 \sinh b,$$

$$m_{I7} = \frac{\sinh a\ \sin\sqrt{R_I}}{a} - \frac{\cosh a\ \cos\sqrt{R_I}}{\sqrt{R_I}}\quad m_{I4} = \frac{\sin\sqrt{R_I}\ \cosh a}{a} - \frac{\sinh a \cos\sqrt{R_I}}{\sqrt{R_I}},$$

$$m_{I5} = (3\cosh a - a\sinh a)\frac{\cos\sqrt{R_I}}{a\sqrt{R_I}} + (1 - A_9)\sinh a\ \sin\sqrt{R_I} + \frac{\cosh a\ \sin\sqrt{R_I}}{a}$$

$$m_{I6} = (3\sinh a - a\cosh a)\frac{\cos\sqrt{R_I}}{a\sqrt{R_I}} + (1 - A_9)\cosh a\ \sin\sqrt{R_I} + \frac{\sinh a\ \sin\sqrt{R_I}}{a}$$

5. Result and discussion

The effects of linear, parabolic and inverted parabolic temperature profiles on DBM convection in a single component composite system with variable heat sources are investigated. The thermal Marangoni number (TMN) is obtained for lower rigid and upper free horizontally bounded surfaces with thermally adiabatic conditions by

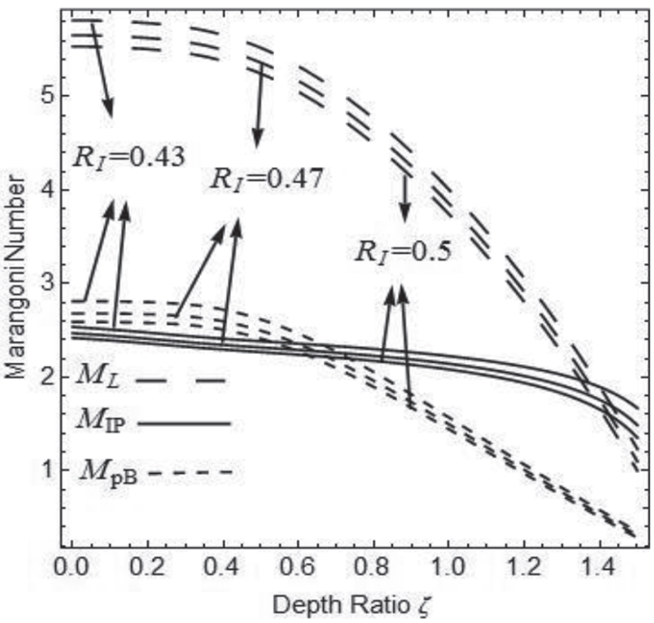

Figure 1: Effects of RI

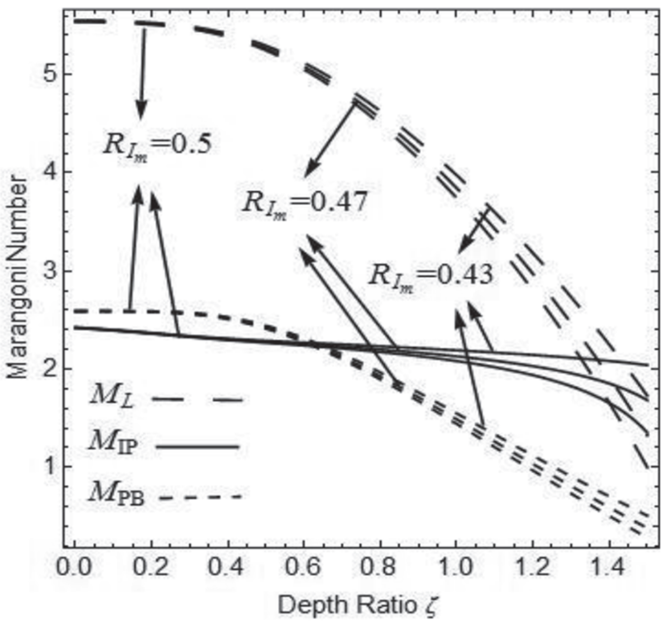

Figure 2: Effects of R

using exact method. Corresponding TMNs, M_L (linear), M_{PB} (parabolic) and M_{IP} (inverted parabolic) against depth ratio ζ for some fixed parameters are shown graphically. When comparing the temperature profiles, the observation shows that the linear profile has a higher TMN, indicating that it is the most stable profile, the most unstable profile is the inverted parabolic profile, as shown in Figures 1, 2, 3, and 4 with $M_{IP} < M_{PB} < M_L$ for lower values of the depth ratios, that is, for the porous layer dominant (PLD) composite system and $M_{PB} < M_L < M_{IP}$ for higher values of the depth ratios.

The effect of R_I = 0.43, 0.47, 0.5 in the fluid layer, on DBM convection, for a set of fixed physical parameters $R_{I_m} = \varepsilon_T = 0.5$, $a = 1$, $\hat{\mu} = 1$, and $Da = 10$ is shown in Figure. 1. It can be observed that Marangoni numbers M_L, M_{PB}, and M_{IP} are higher for smaller depth ratio ζ values and then gradually decrease with further increase in ζ. Also as R_I increases, the TMN M_L, M_{PB}, and M_{IP} decreases, thus destabilizing the system. This indicates that the smaller values of this parameter are suitable to control DBM convection. The effect of R_I on the eigen value is parallel for all the three profiles and is uniform for all the ζ values.

The TMN versus ζ for the supplement parameters, $R_I = \varepsilon_T = 0.5$, $a = \hat{\mu} = 1$, $Da = 10$, and various values of R_{I_m} = 0.43, 0.47, 0.5 are shown in Figure 2. Increase in R_{I_m} decreases TMN in all three profiles and thus destabilizes the system. Also the diverging curves depict that the effect of R_{I_m} is more for higher values of ζ, that is, it is effective for fluid layer dominant (FLD) composite systems. The smaller values of internal Rayleigh number are suitable to control DBM convection for the chosen set of parameter.

The effect of ε_T for a set of fixed values $R_I = R_{I_m} = 0.5$, $Da = 10$, and $\hat{\mu} = a = 1$ and for ε_T = 0.36, 0.38, 0.4 are depicted in Figure 3. The ε_T value is higher for smaller depth ratio and gradually decreases as ζ increases. It is observed that the TMN for all the profiles considered decreases as ε_T increases, as a result, the system is destabilized. In addition, the converging curves show that in PLD composite systems, the effect is significant.

To analyze the permeability on the onset of DBM convection in the porous layer, we have plotted in Figure 4, the values of TMN as a function of ζ, considering different values of Da = 10, 20, 100 and $R_I = R_{I_m} = \varepsilon_T = 0.5$ and $a = \hat{\mu} = 1$. It is seen that increase in Da decreases the TMN in all three profiles and thus enhancing the onset of DBM convection.

The effects of 'a' for the fluid layer on the TMN when $R_I = R_{I_m} = \varepsilon_T = 0.5$, $Da = 10$, $\hat{\mu} = 1$ are shown in Figure 5 while a = 1.18, 1.19, 1.2. We observe that TMN increases as wave number increases in all three profiles thus stabilizing the system. Physically, the size of the convection cells decreases as the wave number increases.

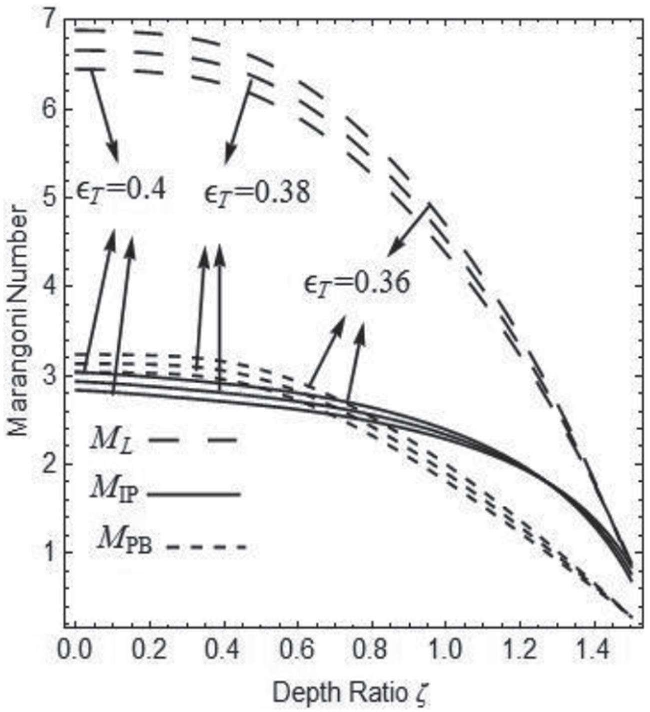

Figure 3: Effects of ε_T

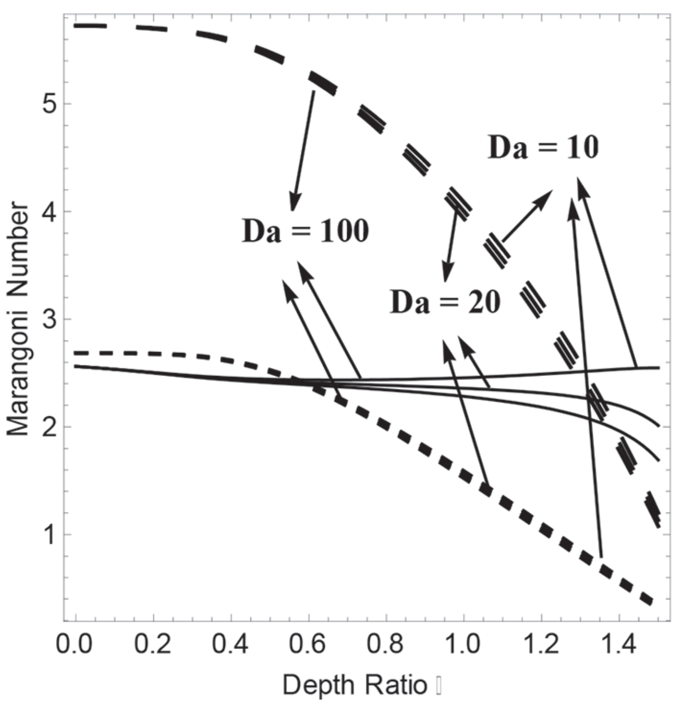

Figure 4: Effects of Da

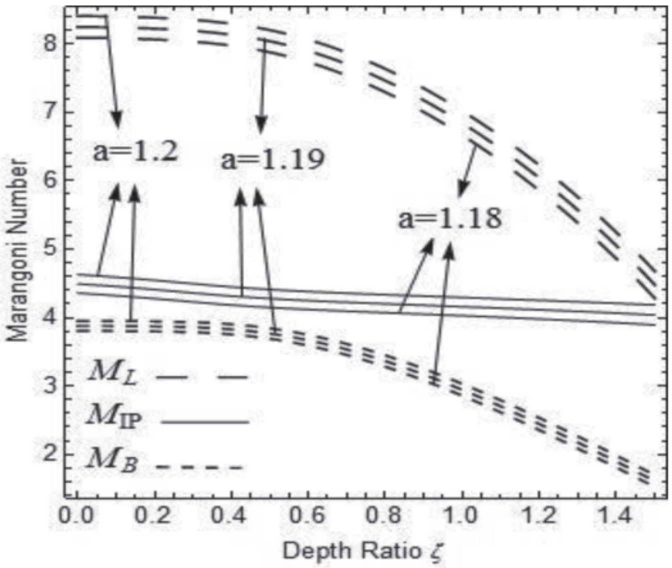

Figure. 5: Effects of *a*

6. Conclusion

The effects of uniform and non-uniform temperature profiles on the onset of DBM convection in a single component composite system with variable heat sources is studied analytically by exact method. The following are the findings:

1. The comparison of TMNs from the graphs show that linear profile is the most stabilizing basic temperature profile. As a result, this profile can be used to effectively control the DBM convection.
2. $M_{IP} < M_{PB} < M_L$ for porous layer dominant composite layer systems and $M_{PB} < M_L < M_{IP}$ for a composite system with a fluid layer dominating.
3. The eigen value, TMN decreases, that is DBM convection can be preponed with increase in values of R_I, R_{Im}, Da and ε_T.
4. The TMN increases, that is, DBM convection can be postponed with increase in wave number *a*.
5. The heat source's strength has a significant impact on DBM convection which either stabilizes or destabilizes the system depending on various other parameters chosen.

References

[1] Kuznetsov, A.V., Nield, D.A. (2016). The effect of spatially nonuniform internal heating on the onset of convection in a horizontal fluid layer. ASME. J.Heat Transfer, 138(6), 062503: 1- 9.

[2] Mokhtar, N.F.M et al. (2011). Effect of heat generation on the onset of Marangoni convection in superposed layers of fluid and saturated porous medium. International Journal of Pure and Applied Mathematics, 67(4), 387-405.

[3] Nanjundappa Rudraiah, Pradeep G. Siddheshwar. (2000). Effect of non-uniform basic temperature gradients on the onset of Marangoni convection in a fluid with suspended particles. Aerospace Science and Technology, 4(8), 517-523.

[4] Nield, D. A., Kuznetsov, A.V. (2016). The onset of convection in a horizontal porous layer with spatially non-uniform internal heating. Trans.Porous.Med, 111, 541-553.

[5] Pearson, J.R. (1958). On convection cells induced by surface tension. Journal of Fluid Mechanics. 4, 489-500.

[6] Ramachandramurthy, V., and aruna, A.S. (2018). Rayleigh-Benard-Taylor convection in temperature-sensitive Newtonian liquid with heat source. International Journal of Engineering Research and Technology. 7(7), 166-170.

[7] Riahi. N. (1984). Nonlinear convection in a horizontal layer with an internal heat source. Journal of Physical Society of Japan. 53(12), 4169-78.

[8] Shah, Y.T., Andras Szeri. (1974). Marangoni instability in case of a non-uniform heat source. International Journal of heat and Mass Transfer. 17(11), 1419-21.

[9] Shivakumara, I.S., Rudraiah, N., Nanjundappa, C.E. (2002). Effect of non-uniform basic temperature gradient on Rayleigh-Benard-Marangoni convection in ferrofluids. Journal of Magnetism and Magnetic Materials, 248(3), 379-395.

[10] Shivakumara, I.S., Suma, S.P., Gangadharaiah, Y.H. (2011). Effect of non-uniform basic temperature gradients on Marangoni convection with a boundary slab of finite conductivity. International Journal of Engineering Science and Technology. 3(5), 4151-60.

[11] Siti Suzilliana Putri Mohamed Isa et al. (2009). Effects of non-uniform temperature gradients on Marangoni convection with free slip condition. American Journal of Scientific Research(1). 37-44.

[12] Sumithra, R., Archana, M.A., Vanishree, R.K. (2020). Darcy-Benard surface tension driven convection in a composite layer with temperature dependent heat source. Malaya Journal of Mathematik. 8(4), 2074-81.

[13] Sumithra, R., Shyamala Venkatraman. (2020).

Effects of uniform and non-uniform heat profiles on Darcy-Benard-Marangoni convection in a composite layer comprising of couple stress fluid. Malaya Journal of Mathematik, 8(4), 2215-27.

[14] Sumithra, R., Vanishree, R.K., Deepa R Acharya.(2020) Non-Darcian Benard Marangoni Convection in a superposed fluid-porous layer with temperature dependent heat source. Malaya Journal of Mathematik, 8(4), 2233-42.

[15] Sumithra, R., Vanishree, R.K., and Manjunatha, N. (2020). Effect of constant heat source/sink on single component Marangoni convection in a composite layer bounded by adiabatic boundaries in the presence of uniform & non uniform temperature gradients. Malaya Journal of Matematik. 8(2), 306-313.

[16] Vanishree, R.K., Sumithra, R., and Manjunatha, N. (2020). Effect of uniform and non uniform temperature gradients on Benard-Marangoni convection in a superposed fluid and porous layer in the presence of heat source. Gedag & Organisite Review. 33(2), 746-758.